Interactive Effects of Zinc and Titanium Nanoparticles of Leaf Decomposition in Freshwater Ecosystems

Nawal Al Jabri
Sultan Qaboos University
Raeid M.M. Abed
Sultan Qaboos University
Abdulkadir Elshafie
Sultan Qaboos University
Michael J. Barry (mjbarry@squ.edu.om)
Sultan Qaboos University

Research Article

Keywords: Nanotoxicology, interaction, antagonism, ecosystem function

Posted Date: May 5th, 2023

DOI: https://doi.org/10.21203/rs.3.rs-2878460/v1

Additional Declarations: No competing interests reported.

Abstract

In conclusion, we observed that titanium nanoparticles inhibited leaf decomposition more strongly than zinc nanoparticles, and that the combination treatments reduced the effects of the titanium. This was opposite to what we initially expected. The nano-titanium reduced bacterial growth, suggesting that this may be one mechanism that could inhibit decomposition. Light may play a role in generation of reactive oxygen species that increase toxicity of the nanoparticles, but effects are complex. Overall, this study highlights the importance of testing the effects of mixtures that are likely to occur in the environment. Metallic nanoparticles are an emerging hazard that will continue to grow as their use expands in the future.

Zinc and titanium nanoparticles are used in many consumer and industrial products. Consequently, they are increasingly being detected in the sediments of aquatic ecosystems. Despite their frequent co-occurrence, there is little information on how they interact, although previous studies on cells suggest that nano-titanium may inhibit nano-zinc toxicity by reducing Zn^{2+} bioavailability. Leaf decomposition is a major source of allochthanous energy in freshwater ecosystems. In this study we measured the effects of zinc and titanium nanoparticles, alone or in combination, on the rate of leaf decomposition.

In Experiment 1, leaf discs, produced from senescent leaves of *Ficus sycomorus* were exposed to either 1, 10 or 100 mg/L of either ZnO or TiO2 nanoparticles, alone or in combination, for six weeks. Mass loss and microbial metabolism were measured at fortnightly intervals and bacterial community composition measured after six weeks using next generation Illumina MiSeq sequencing. In Experiment 2, *F. sycomorus* leaf discs were exposed for two weeks to10 mg/L ZnO or TiO2 nanoparticles, alone or in combination, both in the light or dark, and in presence or absence of chloramphenicol, a broad spectrum antibacterial, giving a total of 16 treatments. Mass loss, bacterial colony formation, and the C:N ratio of leaf tissue were measured.

In experiment 1 there was no evidence that titanium nanoparticles reduced the concentration of Zn^{2+}. After six weeks, there was significantly less mass loss in all titanium nanoparticle treatments, compared with controls, zinc nanoparticles alone, or the combination treatments. Microbial metabolism was initially low, but increased after four weeks, but there were no clear effects of the nanoparticles on oxygen consumption by the microbes. After six weeks, the bacterial communities of leaves treated with 10 and 100 mg/L of the combination treatment and the 100 mg/L zinc nanoparticle treatments, showed a clear separation from other treatments int terms of community composition. The dominant species in the three communities was *Bacillus subtillus.* In experiment 2, there was greater mass loss in the dark and lower mass loss in treatments containing chloramphenicol. Both nano-titanium and chloramphenicol inhibited bacterial growth, but there were complex three-way interactions between all three factors. The C:N ratio was lowest in controls and highest in the leaves exposed to nano-titanium. There was also an interaction between light and nanoparticle treatment.

Introduction

Metallic nanoparticles are widely used in consumer products including sunscreens, textiles, paints and cosmetics (Mody et al. 2010). These nanoparticles can reach the environment through runoff after rainfall, through the waste water system, and from direct contact with water (Rajput et al. 2020). Ultimate sinks for nanomaterials are likely to be lakes, streams and near-shore environments (Arienzo and Ferrara 2022). Metallic nanoparticles pose particular risks to ecosystems due to their ability to exert toxicity through multiple mechanisms including release of metallic ions, production of reactive oxygen species (ROS) and through physical damage to cells (Venkatasubbu et al. 2016; Slavin et al. 2017; Zhang et al. 2018; Medici et al. 2021). As the use of nanoparticles continues to grow, it is predicted that sediment concentrations of nano-TiO_2 will reach 6.7–40,000 µg/kg while nano-ZnO2 will be somewhat lower but still substantial (Sun et al. 2016).

Leaf decomposition is the major source of allochthanous energy in many stream ecosystems (Abelho, 2001, Tank et al. 2010, Benbow, 2020, Swan et al. 2021). Decomposition is a complex process involving loss of soluble colloids, colonization by microbes, and finally physical fragmentation or consumption by macroinvertebrates. The nutrients and energy released by decomposition are transported downstream to lower river reaches, horizontally to the floodplain, or stored vertically in the benthos (Robertson et al., 1999). Any alteration to the natural sequence of decomposition has capacity to cause disturbance to all parts of the ecosystem. Leaf decomposition is sensitive to a range of pollutants including fungicides, pesticides, and metals (Pradhan et al. 2011). Metallic nanoparticles may also impact the decomposition process. Previous studies show that both nano-Ti (nT) and nano-Zn (nZ) reduced the rate of leaf decomposition and that the effects of nano-Ti were strongest in the dark (Al Riyami et al, 2019). Similarly, nano-Zn decreased the activity of soil bacterial communities (Rashid et al. 2017), while low concentrations of nZ (< 300 µg/L) initially promoted but later suppressed fungal biomass during leaf decomposition (Du et al. 2020). In another study, it was found that fairly high concentrations of nZ (100 mg/L) inhibited leaf decomposition in aquatic microcosms (Du et al. 2019). While three different sizes of nZ inhibited poplar leaf decomposition at 100 mg/L (Du et al. 2017), and nT enhanced the decomposition of *Typa* leaves over the long term by promoting fungal biomass and activity (Zhang et al. 2019).

Although, nZ and nT share many similarities including band gap and band energies (Buchman et al. 2019), their main mechanisms of toxicity differ. Nano-zinc is inherently unstable and the main environmental concern focuses on release of Zn^{2+} ions (Sirelkhatim et al. 2015). However, nZ effects can also be increased by light (Sivakumar et al. 2018), indicating phototoxicity. In contrast, nT is relatively insoluble and toxicity is mainly related to induction of ROS. Several studies have investigated the joint toxicity of the two nanoparticles with conflicting results. For instance, nano-Ti reduced toxicity of nZ to primary epidermal keratinocytes by adsorbing and immobilizing free Zn^{2+} ions (Kathawala et al. 2015). A similar kinetic model was also demonstrated in Lake Michigan water (Tong et al. 2014). Both studies also described reciprocal inhibition where nZ reduced the toxicity of nT to bacterial cell walls by reducing contact between the cell and titanium. In contrast, a combined nZ + nT particles showed greater toxicity on the fungus *Aspergillus flavus*, than either nanoparticle alone (Najibi Ilkhechi et al. 2021).

Since leaf decomposition involves multiple mechanisms, including physical weakening of the leaf, chemical leaching and colonization by microbes, both nZ and nT may affect these processes in different ways, yet little is known of how they may interact. Based on previous research, we hypothesized that there may be both additive and antagonistic interactions between the two nanoparticles. Specifically we hypothesized:

1. Both nZ and nT alone would decrease the rate of leaf decomposition
2. The presence of nT would decrease the concentration of soluble Zn
3. Combined exposure would have an antagonistic interaction due to reduction in zinc ions

Methods

General

Preparation of leaf discs

Senescent leaves of *Ficus sycomorus* were collected from a single tree in Muscat, Oman. The leaves were washed with tap water and allowed to air dry. Leaf discs, 17 mm in diameter, were made by punching the leaves with a metallic circular drill piece while avoiding the stem or any damaged tissue. The discs were dried for seven days in an oven at 80°C, then weighed to the nearest 0.1 mg to determine the average initial weight. Sets of 70 leaves discs were placed into mesh bags (20×20 cm and 0.5 mm pore size), then submerged to a depth of 0.5 m in a small flowing stream (Wadi Sa'al: 23º31 60 N and 58º12 0 E) and left for one week to allow microbial colonization. After one week, the mesh bags were retrieved and the leaf discs were rinsed with distilled water.

Preparation of nanoparticles

Stock nanoparticle solutions of ZnO_2 (nZ) (Sigma®, 21 nm) and TiO_2 (nT) (Sigma®, 10–30 nm) were prepared by adding 3, 30 or 300 mg of the required nanoparticles (NP) to 100 mL of deionized water. The NP solutions were sonicated for 30 min at 50 W and 40 KHz then mixed with 2.9 L of freshly collected wadi water to give final concentrations of 1, 10 or 100 mg/L. The combination treatments were prepared by mixing 3, 30 or 300 mg of each NP in 100 mL of deionized water. The solutions were then combined and sonicated before adding to 2.8 L of wadi water.

Verification of nanoparticles

Dynamic Light Scattering (DLS): The particle size of nanoparticles was measured by laser diffraction using a Nano Size Particle Analyzer (Zen 1600 Malvern, USA) for range in between 0.6 nm and 6.0 µm. with the following conditions: temperature 25°C, particle refractive index 1.590, water refractive index 1.33 and particle absorption coefficient 0.01. Three measurement cycles were recorded and the data were averaged by a software (DTS, Ver.5.00, Malvern®). Analysis was done for all nine treatments in order to get the actual size of the nanoparticles.

Scanning Electron Microscope (SEM): The morphology and size of nZ and nT nanoparticles were also verified by SEM (Joel JSM-7600F).

Experiment 1: Effect of NP on leaf decomposition and microbial communities

The experimental treatments were prepared by adding 550 mL of NP solution or water control to circular transparent polypropylene containers. There were a total of ten treatments: control, 1 mg/L nZ (Z1), 10 mg/L nZ (Z10), 100 mg/L nZ (Z100), 1 mg/L nT (T1), 10 mg/L nT (T10), 100 mg/L nT (T100), or 1 + 1, 10 + 10 and 100 + 100 mg/L nZ + nT (TZ1, TZ10 and TZ100) respectively. Each treatment was replicated nine times and six pre-incubated leaf discs were added to each container. The containers were randomly distributed on a balcony where they were exposed to indirect sunlight. At weekly intervals T, O_2, pH and conductivity were recorded and evaporative loss replaced with deionized water. At one, three and five weeks after the start of the experiment a 45 mL composite sample was taken from each of the treatments (15 mL from three replicates), filtered through Whatmans No 41 filter paper and the volume made up to 50 mL with deionized water before analysis of metal ions using by ICP-MS (Make-Bruker-Arora M90).

Two, four and six weeks after the start of the experiment, three replicates were removed and two leaves were haphazardly selected from each replicate, dried for 72 h at 80°C, then weighed to nearest 0.1 mg. Percentage mass loss of each leaf was calculated. Microbial metabolism was used as a surrogate measure of microbial biomass and was measured at the same time intervals of two, four and six weeks. A single leaf disc from each of three replicates was placed in 10 mL glass vials filled with oxygen-saturated water. An additional three vials without leaf discs were also prepared to measure background respiration. The vials were sealed and placed in a water bath (25 ± 1°C) for 24 h. The entire system was kept in the dark. After the incubation, water was removed from the vials with a syringe and slowly injected into another tube where the oxygen concentration and temperature were recorded with an optical sensor attached to a FireSting® oxygen meter (PyroScience, GmbH, Germany). The sensor was calibrated with 100% saturated water and a zero solution (sodium dithionate) before each recording session. After measurement, the leaves were retrieved from the tubes and dried at 80°C for 72 h to determine their dry mass.

The following equation was used to calculate the respiration rate in mg O_2/h:

$((O_b - O_f))/m \div 24$

Ob: Average oxygen concentration in blank vials after 24 h incubation

Of: Oxygen concentration of sample after 24 h incubation

m: Leaf disc dry mass

The bacterial community composition was determined after six weeks. Pooled samples were prepared by haphazardly selecting a single leaf disc from each of the three remaining replicates of each treatment. The discs were placed in sterile Eppendorf tubes and immediately stored at -4°C in a refrigerator until DNA extraction. Bacterial DNA was extracted from the leaf samples following the protocol Smalla et al. (1993) with minor modifications. The concentration and purity of the DNA was tested using NanoDrop®. The purified DNA was analyzed using paired-end Illumina MiSeq sequencing (MRDNA, Texas, USA) of the bacterial 16S rRNA genes for bacterial sequences.

Experiment 2: direct and indirect effects of NP

The aim of this experiment was to identify direct physical effects of the nanoparticles from indirect effects due to production of ROS and toxicity to the microbial community. Stock solutions of nanoparticles and freshly collected Wadi Sa'al water were prepared using methods described in Experiment 1. Two hundred milliliters of solution was added to each of 48–250 mL Erlenmeyer flasks. The flasks were divided into four nanoparticle treatments, each replicated 12 times: control, 10 mg/L nZ (Z10), 10 mg/L nT (T10) or 10 mg/L nZ + 10 mg/L nT (TZ10). One 10 µg disc of the antibiotic chloramphenicol (Thermo Scientific® OXIOD, CT0012B, Hampshire, England) was added to half the flasks. Chloramphenicol is a broad spectrum bacterial inhibitor that also shows effects towards fungi. Four freshly prepared *F. sycomorus* discs (see Exp. 1) were added to each flask and the flasks placed on a north facing balcony to receive indirect sunlight. Half the flasks were covered with sheets of black cardboard to prevent exposure to light, giving a total of 16 treatments, each replicated three times (Table 1). The flasks were stirred daily by swirling. After seven days, a 10 mL water sample was taken from each flask for measurement of metal ions. At the same time pH, temperature and conductivity were also measured. After 14 days, the leaf discs were recovered by carefully pouring the contents into a Petri dish. One leaf disc was haphazardly selected for mass loss, while another selected for carbon, nitrogen and hydrogen analysis Perkin Elmer® CHNSO analyzer), and another for bacterial colony forming unit (CFU) counts. Bacterial counts were determined by adding 0.3 g of leaf to sterile distilled water and vortexing for one minute. The sample was serially diluted until a dilution of 10^{-5} was reached. The diluted samples were spread on nutrient agar (two petri dishes). All petri dishes were incubated for 3 days and the number of colonies was counted.

Table 1. Design for Experiment 2

Light								Dark							
- Chloramphenicol				+ Chloramphenicol				- Chloramphenicol				+ Chloramphenicol			
C[1]	nZ[2]	nT[3]	nTZ[4]	C	nZ	nT	nTZ	C	nZ	nT	nTZ	C	nZ	nT	nTZ

[1]Control, [2]10 mg/L nZ. [3]10 mg/L nT, [4]10 mg/L nZ+10 mg/L nT

Data Analysis:

In experiment 1, the effects of nanoparticle treatment on leaf mass loss and microbial metabolism were analyzed by one-way generalized linear models. The effects of nanoparticle treatment on bacterial community diversity were analyzed by cluster analysis of OTUs using Bray-Curtis dissimilarity. In experiment 2, the effects of nanoparticle treatment, light and antibiotic exposure on leaf mass loss, bacterial colony formation and C:N ratio were analyzed by three-way generalized linear models. Data was assessed for normality and heteroscendacity before analysis and if necessary log-transformed and reassessed. Significant factors and interactions were assessed using pairwise comparisons with a sequential Bonferroni correction. Analyses were perform in SPSS (v21) except cluster analysis which was performed in Past (v4.05 Hammer at al., 2001). All results are reported as mean ± 1 SE. $P < 0.05$ is considered significant.

Results

Exp.1.

Physico-chemical parameters ranged between 5.0-10.1 mg/L (O_2), 920–2116 µS (conductivity) and 7.99–8.95 (pH), but there were no differences between treatments. Dissolved ionic Zn^+ concentrations were correlated with nanoparticle densities and peaked in Week 1 before declining sharply (Fig. 1). After one week, there was no evidence that the presence of nT decreased the concentration of ionic Zn at 100 mg/L. However, after five weeks, the concentration was higher in the nZ treatments compared with the nZT. On the other hand, the concentration of Zn2 + ions in the nZ treatment was higher than in the nZT ones after one week, but the difference was not significant by the end of the experiment.

The size distributions for nZ by DLS were 176.7–370.0 nm (Z1), 596.0-1135.1 nm (Z10) and 366.0-771.2 nm (Z100) (Appendix 1) For nT size distributions were 29.7-115.2 nm (T1), 45–100 nm (T10) and 1236.1-2853.2 nm (T100) (Appendix 1). Sizes based on SEM were 40 nm for nZ and 30 nm for nT (Appendix 1).

After 14 days incubation, the highest average leaf mass loss was 70.9 ± 4.7% in controls and the lowest was 40.3 ± 14.39% in the TZ100 (GLM $P = 0.020$, Fig. 2A). Pairwise contrasts showed that the only a significant difference was between the controls and TZ100 treatment. Overall, microbial metabolism was low, indicating small amounts of bacterial activity. However, microbial metabolism was highest in the TZ treatments ($P < 0.0001$, Fig. 3A), with all TZ combination and the T100 treatments having significantly higher metabolic rates than controls. There was no correlation between percentage leaf mass loss and metabolic rate (Pearson Correlation: -0.109, $P = 0.566$, $N = 30$).

After 28 days, the highest leaf mass loss was in the T1 and Z100 treatments and lowest in the T10 treatment ($P = 0.002$, Fig. 2B). However, pairwise comparisons could not distinguish any significant differences. Microbial metabolism peaked at 28 days and was 10-100x greater than on day 14. There was an overall significant difference in metabolic rate between treatments ($P < 0.0001$, Fig. 3B). As on day 14, highest rates were in the TZ treatments and the lowest were in the T10 treatment, but pair-wise comparisons did not show specific differences. Again there was no correlation between percentage leaf mass loss and microbial metabolic rate (Pearson Correlation: 0.0289, $P = 0.865$, $N = 30$).

On day 42, highest mass loss was in the Z1 treatment, and lowest in the all the TZ treatments ($P < 0.001$, Fig. 2C). The metabolic rate was lower than on day 28, but still higher than on day 14. The highest values were now in the Z1 and Z10 treatments ($P = 0.009$, Fig. 3C), but were not significantly different from the controls. After 42 days, there was a strong correlation between percentage mass loss and metabolic rate (Pearson Correlation: 0.536, $P = 0.002$, $N = 30$). There was also an overall correlation between percentage mass loss and metabolic rate pooling over all weeks (Pearson Correlation: 0.405, $P < 0.001$, $N = 90$).

Bacterial community analysis:

Cluster analysis of OTUs using Bray-Curtis dissimilarity revealed the formation of two distinct clusters, one includes the samples exposed to TZ10, TZ100 and Z100, while the other includes the remaining samples (Fig. 4). The control treatment was mainly dominated by sequences belonging to the phyla Proteobacteria and Actinobacteria. The proteobacterial sequences were more or less equally distributed among the classes, Alpha-, Gamma- and Betaproteobacteria. The dominant OTUs in the control sample belonged to the genera *Delftia*, *Pseudomonas* and *Propionibacterium*. After exposure to Z1 and Z10, the proportion of Alphaproteobacteria decreased from 30% to ≤ 2% of total sequences, whereas the proportion of Bacilli and Gammaproteobacteria increased to reach ca. 13% and 39% of total sequences in each treatment, respectively. The detected OTUs (OTUs 2, 3, 4, and 7) were similar to the control, but at higher proportions. In the Z10, the relative abundance of Acidobacteria reached ca. 35% of total sequences. Upon exposure to Z100, the relative abundance of Betaproteobacteria, Cytophagia and Flavobacteria increased when compared to the control while the propotion of Alphaproteobacteria, Gammaproteobacteria and Actinobacteria were lower.

Exposure to different concentrations of nT also showed differences in bacterial communities. Exposure to T1 and T10 resulted in a decrease in the relative abundance of Alphaproteobacteria, but an increase in Bacilli, while the remaining dominant groups like Gammaproteobacteria, Betaproteobacteria, and Actinobacteria remained more or less at comparable proportions. The most commonly detected OTUs in these treatment were related to the genera *Delftia*, *Pseudomonas*, and *Propionibacterium*. A major change in the bacterial community was observed after exposure to T100, with ca. 96% of the sequences belonging to Bacilli. This dominance of Bacilli was also observed when the leaves were exposed to TZ1 and TZ100. More than 86% of all OTUs in these treatments belonged to *Bacillus subtilis*. Exposure to TZ10 resulted in a bacterial community dominated mainly by Actinobacteria (30% of total sequences), Flavobacteria (18%), and Clostridia (10%). Clostridia were only detectable in this treatment as well as the highest proportion of the OTU14 belonging to *Cloacidobacterium normanense*. Alpa-, Gamma- and Proteobacteria decreased in relative abundance in this treatment.

Exp.2.

The concentration of Zn^{2+} ions ranged between 20 and 990 µg/L. The lowest value was in the nZT treatment in light, without antibiotic. The main water parameters were as follows: pH 7.92–8.77, temperature week 1: 23.5-24.9°C; week 2: 21.4-22.7°C. Temperatures were slightly warmer in the light

exposed tubes. Conductivity: 1900–2100 µS/cm. Light intensity week 1: 2516 Lux and week 2: 1960. DLS showed a diameter for the ZnO-NPs 221 nm ± 132–324 while for TiO_2-NPs it was10 nm ± 8–12 (Appendix 2). TEM images of TiO_2-NPs showed average size for Ti-NPs 51.14 nm ± 5.98 nm and ZnO-NPs 66.19nm ± 11.66 (Appendix 1).

There was an overall effect of NP treatment on leaf mass loss (P = 0.0.013, Fig. 5A), with highest loss for nZ and lowest for nZT, but no treatment was significantly different from the controls. There was a strong effect of light with greater mass loss in the dark (P < 0.0001) and of antibiotic treatment (P = 0.002), with the chloramphenicol decreasing the mass loss. There was also an interaction between antibiotic exposure and NP treatment (P = 0.001). Controls exposed to chloramphenicol had significantly lower mass loss than antibiotic-free controls. However, there was also a significant three-way interaction (P = 0.01, Fig. 5B-D). Mass loss was significantly higher for the controls without antibiotics in the light compared with the controls with antibiotics in the light (Fig. 5B). Also in the presence of antibiotic, control mass loss was lower in the light compared to the dark, which was opposite to all the nanoparticle groups. In contrast, for the nZ and nT treatments, mass loss was lower in the dark with antibiotic than in the light (Figs. 5C, D). Finally, for nT without antibiotic, mass loss was lower in the light compared with the dark (Fig. 5E).

Bacterial counts were obtained from all samples except two: one nT light treatment and one from nZ antibiotic-dark treatment where there was some contamination. There was a direct effect of the nano-treatment on CFU counts with lowest numbers in the nT treatment (P < 0.001, Fig. 6B). There was also an inhibitory effect of antibiotic treatment (P = 0.006), but also a three-way interaction between light, antibiotic and nanoparticle treatments (P = 0.009). Contrasts showed that the CFU count was significantly higher in the dark-nZ treatments without antibiotics compared to with them. The opposite pattern was observed for nZ in the light. There was also significant differences in CFU between light and dark for nZ and nT with antibiotics (Figs. 5D-F).

There was an effect of NP treatment on the C/N ratio of the leaves with the highest ratio in nT treatment and the lowest in the controls (P = 0.001, Fig. 6A). There was a direct effect on chloramphenicol with a higher C/N ratio in the untreated leaves (P = 0.007). Finally there was an interaction between treatment and light (P = 0.019). Pairwise comparisons showed that it was due to a significantly low C/N ratio in the control leaves compared to the control + chloramphenicol ones.

Discussion

For two decades environmental scientists have warned of the potential risks that manufactured nanomaterials will pose once they reach a critical threshold in the environment. Increasing production of nanomaterials and their incorporation into new products has now turned these warnings into reality, as particles reach the environment and accumulate in sediments, where they have the ability to circulate throughout the aquatic environment (Sharma, 2009, Asztemborska et al. 2018).

Most previous studies have focused on single NP types and little is known about how multiple NP types will interact with each other and with complex environmental matrices. Noticeably, there is conflicting evidence on the joint toxicity of nano-ZnO_2 and nano-TiO_2 with both additive and antagonistic interactions reported. We measured the effects of the two nanoparticle types on leaf decomposition, because it is key process in stream ecosystem function. As zinc NPs are generally regarded as more toxic than titanium ones, we expected the strongest inhibition of decomposition in the nZ treatments. If the nano-zino and -titanium had an antagonistic interaction we expected less inhibition in the nZT microcosms compared with nZ alone. However, at the end of experiment 1, it was clear that the lowest decomposition had occurred in the nT treatments, although the decomposition rate also decreased with increasing nZ concentration. Decomposition in the nZT treatment was similar to controls, supporting an antagonistic model. However, we observed that the presence of nZ particles reduced the effects of nT, rather than the other way around, although such a conclusion depends on the timescale observed. In experiment 1, microbial activity was low in all treatments after 14 days incubation, although slightly elevated in the mixed NP treatments compared to controls. This suggests that most of the initial decomposition was due to loss of labile cell contents and physical weakening of leaf structure. Microbial activity increased by an order of magnitude after 28 days in all treatments but subsided again after six weeks, remaining slightly elevated in the controls and nZ1 and nZ10 treatments. Previous studies have suggested that nT can bind ionic nZ, hence reducing its bioavailability (Tong et al. 2014), but our data shows that there was only a significant reduction in Zn^{2+} at 100 mg/L in the nZT treatment, but not at 1 or 10 mg/L. In fact after seven days at 1 mg/L, the Zn^{2+} concentrations were higher in the nZ alone compared with the ZT treatment. However, in all treatments, ionic Zn decreased rapidly and by 21 days was < 500 µg/L. Most studies suggested that the toxicity threshold for Zn^{2+} is above 1 mg/L (Ghosh et al. 1996; Paulsson et al. 2000).

Although some studies argue that most, if not all toxicity from Zn NP is due to ionic Zn^{2+} (Bacchetta et al. 2016), impacts such as generation of ROS and direct membrane damage are also possible, but usually require contact with the bacterium membrane (Neal 2008; Hou et al. 2018). In contrast, titanium NP are regarded as effectively insoluble (Mbanga et al. 2022), so most toxicity is expected to be from direct contact and generation of ROS.

In terms of the bacterial community composition, we observed that TZ10, 100 and Z100 treatments created a cluster that was quite separate from the other treatments. There was a noticeably higher abundance of Bacilli in the T100, TZ1, and TZ100 treatments, but a relatively lower density in the TZ10. The functional roles of bacteria in leaf decomposition are still largely unknown (Zhou et al., 2017), but bacilli can produce cellulose and play a significant role in leaf decomposition (Prince et al., 2010). On the other hand Gammaproteobacteria, Actinobacteria, and Betaproteobacteria dominated in the control and low nZ treatments. Bacterial communities are often quite dynamic with intense competition for resources (Moitinho et al., 2018). If the Gammaproteobacteria, Actinobacteria, and Betaproteobacteria were more susceptible to nanoparticles, they may have been inhibited, allowing the Bacilli to dominate. Our poor understanding of the sensitivity and functional role individual microbial species remains a major

roadblock on the path to understanding the effects of chemical stressors on functional ecosystem processes. One limitation of our microbial analysis is that we didn't measure fungal diversity, although previous studies suggest that fungal biomass tends to be low in Omani wadis (Al Riyami et al., 2009, Al Riyami et al., 2019).

In the second experiment, we expected the addition of an antimicrobial compound to decrease decomposition as it would inhibit microbial degradation of the leaves. This occurred for the controls in the light. However, the effect of chloramphenicol in the nZ and nT microcosms was strongest in the dark, with no effect in the light. In the nZT treatment there was no effect at all of the antibiotic. However, this experiment only ran for 14 days and at the end the lowest rate of decomposition was in the nTZ treatment, which is similar to 14 days in experiment 1. We also observed that the highest C/N ratio in the nT treatment possibly indicating a slower rate of decomposition.

Several previous studies have demonstrated that Zn nanoparticles can affect leaf decomposition (Feckler et al. 2015; Du et al. 2017, 2022; Rashid et al. 2017; Al Riyami et al. 2019). Generally, nano-titanium has been viewed as less toxic, requiring higher densities to cause inhibition compared with nano-zinc (Du et al. 2018), although it was found that 1g/L of titanium NP actually stimulated decomposition (Zhang et al. 2019). It was also found that titanium NPs could inhibit decomposition of *Ficus vastus* leaves in the dark, but not the light at 10 mg/L (Al Riyami et al. (2017). They suggested that in the light, nano-titanium may produce ROS that can damage the leaf structure and enhance decomposition counteracting any loss of microbial decomposers. In this study, we observed the opposite effect, with significantly lower decomposition in the light. Light intensity was lower in the current study averaging 2087 Lux compared with 3309 Lux in Al Riyami et al. (2017). Also water temperature was much higher in the earlier study, around 36°C, as it was run at the peak of summer, which would greatly increase the rate of leaf breakdown.

The decomposition of leaf litter occurs in a complex environmental matrix that includes not just microbes but macroinvertebrates that shred and consume processed leaf litter. For instance, the photocatalytic properties on titanium NP caused amphipods to avoid contaminated leaves in sunlight (Li et al. 2014). Similarly, complex matrices of pollutants can have multiple effects. It is likely that leaf type, microbial community, temperature, pH, nutrient availability and extent light intensity will all interact with nano-pollutants to effect the decomposition process. More information is needed to make meaningful prediction on the ecological risks on metallic nanoparticles in the future.

Declarations

Acknowledgements

The authors declare no conflict of interest. We thank the Central Analytical Unit, College of Science, Sultan Qaboos University for analysis of metal concentrations and SEM of nanoparticles, and the Centre

for nanotechnology, College of Engineering Sultan Qaboos University for DLS measurements. This study was support by a Sultan Qaboos University Internal Grant to MJB.

References

1. Al-Riyami M, Victor R, Seena S et al. (2009) Leaf decomposition in a mountain stream in the Sultanate of Oman. Int Rev Hydrobiol 94:16–28. https://doi.org/10.1002/iroh.20081108
2. Al Riyami SA, Mahrouqi DA, Abed RMM, et al (2019) Direct and indirect effects of zinc oxide and titanium dioxide nanoparticles on the decomposition of leaf litter in streams. Ecotoxicology. https://doi.org/10.1007/s10646-019-02036-y
3. Abelho M (2001) From Litterfall to Breakdown in Streams: A Review. The Scientific World Journal 1:656–680. https://doi.org/10.1100/tsw.2001.103
4. Arienzo M, Ferrara L (2022) Environmental Fate of Metal Nanoparticles in Estuarine Environments. Water 14:1297. https://doi.org/10.3390/w14081297
5. Asztemborska M, Jakubiak M, Stęborowski R, et al (2018) Titanium Dioxide Nanoparticle Circulation in an Aquatic Ecosystem. Water Air Soil Pollut 229:208. https://doi.org/10.1007/s11270-018-3852-8
6. Bacchetta R, Maran B, Marelli M, et al (2016) Role of soluble zinc in ZnO nanoparticle cytotoxicity in *Daphnia magna*: A morphological approach. Environmental Research 148:376–385. https://doi.org/10.1016/j.envres.2016.04.028
7. Benbow ME, Receveur JP, Lamberti GA (2020) Death and Decomposition in Aquatic Ecosystems. Frontiers in Ecology and Evolution 8:
8. Buchman JT, Hudson-Smith NV, Landy KM, Haynes CL (2019) Understanding Nanoparticle Toxicity Mechanisms To Inform Redesign Strategies To Reduce Environmental Impact. Acc Chem Res 52:1632–1642. https://doi.org/10.1021/acs.accounts.9b00053
9. Du J, Zhang Y, Cui M, et al (2017) Evidence for negative effects of ZnO nanoparticles on leaf litter decomposition in freshwater ecosystems. Environmental Science: Nano 4:2377–2387. https://doi.org/10.1039/C7EN00784A
10. Du J, Zhang Y, Guo W, et al (2018) Chronic impacts of TiO2 nanoparticles on Populus nigra L. leaf decomposition in freshwater ecosystem. Journal of Hazardous Materials 350:121–127. https://doi.org/10.1016/j.jhazmat.2018.02.010
11. Du J, Zhang Y, Qv M, et al (2019) The effects of ZnO nanoparticles on leaf litter decomposition under natural sunlight. Environ Sci: Nano 6:1180–1188. https://doi.org/10.1039/C8EN01353E
12. Du J, Zhang Y, Yin Y, et al (2020) Do environmental concentrations of zinc oxide nanoparticle pose ecotoxicological risk to aquatic fungi associated with leaf litter decomposition? Water Research 178:115840. https://doi.org/10.1016/j.watres.2020.115840
13. Du J, Qv W, Niu Y, et al (2022) Nanoplastic pollution inhibits stream leaf decomposition through modulating microbial metabolic activity and fungal community structure. Journal of Hazardous Materials 424:127392. https://doi.org/10.1016/j.jhazmat.2021.127392

14. Feckler A, Kahlert M, Bundschuh M (2015) Impacts of Contaminants on the Ecological Role of Lotic Biofilms. Bulletin of environmental contamination and toxicology 95:421–427
15. Ghosh SK, Doctor PB, Kulkami PK (1996) Toxicity of zinc in three microbial test systems. Environmental Toxicology and Water Quality 11:13–19. https://doi.org/10.1002/(SICI)1098-2256(1996)11:1<13::AID-TOX3>3.0.CO;2-C
16. Hou J, Wu Y, Li X, et al (2018) Toxic effects of different types of zinc oxide nanoparticles on algae, plants, invertebrates, vertebrates and microorganisms. Chemosphere 193:852–860. https://doi.org/10.1016/j.chemosphere.2017.11.077
17. Kathawala MH, Ng KW, Loo SCJ (2015) TiO2 nanoparticles alleviate toxicity by reducing free Zn2+ ion in human primary epidermal keratinocytes exposed to ZnO nanoparticles. J Nanopart Res 17:263. https://doi.org/10.1007/s11051-015-3068-4
18. Li S, Wallis LK, Ma H, Diamond SA (2014) Phototoxicity of TiO2 nanoparticles to a freshwater benthic amphipod: Are benthic systems at risk? Science of The Total Environment 466–467:800–808. https://doi.org/10.1016/j.scitotenv.2013.07.059
19. Mbanga O, Cukrowska E, Gulumian M (2022) Dissolution of titanium dioxide nanoparticles in synthetic biological and environmental media to predict their biodurability and persistence. Toxicology in Vitro 84:105457. https://doi.org/10.1016/j.tiv.2022.105457
20. Medici S, Peana M, Pelucelli A, Zoroddu MA (2021) An updated overview on metal nanoparticles toxicity. Seminars in Cancer Biology 76:17–26. https://doi.org/10.1016/j.semcancer.2021.06.020
21. Mody VV, Siwale R, Singh A, Mody HR (2010) Introduction to metallic nanoparticles. J Pharm Bioallied Sci 2:282–289. https://doi.org/10.4103/0975-7406.72127
22. Moitinho MA, Bononi L, Souza DT, et al (2018) Bacterial Succession Decreases Network Complexity During Plant Material Decomposition in Mangroves. Microb Ecol 76:954–963. https://doi.org/10.1007/s00248-018-1190-4
23. Najibi Ilkhechi N, Mozammel M, Yari Khosroushahi A (2021) Antifungal effects of ZnO, TiO2 and ZnO-TiO2 nanostructures on Aspergillus flavus. Pesticide Biochemistry and Physiology 176:104869. https://doi.org/10.1016/j.pestbp.2021.104869
24. Neal AL (2008) What can be inferred from bacterium–nanoparticle interactions about the potential consequences of environmental exposure to nanoparticles? Ecotoxicology 17:362–371. https://doi.org/10.1007/s10646-008-0217-x
25. Paulsson M, Nyström B, Blanck H (2000) Long-term toxicity of zinc to bacteria and algae in periphyton communities from the river Göta Älv, based on a microcosm study. Aquatic Toxicology 47:243–257. https://doi.org/10.1016/S0166-445X(99)00013-2
26. Pradhan A, Seena S, Pascoal C, Cássio F (2011) Can Metal Nanoparticles Be a Threat to Microbial Decomposers of Plant Litter in Streams? Microbial Ecology 62:58–68. https://doi.org/10.1007/s00248-011-9861-4
27. Prince RC, Gramain A, Mcgenity TJ (2010) Prokaryotic hydrocarbon degraders. Handbook of Hydrocarbon and Lipid Microbiology. 1672–1692. https://doi.org/10.1007/978-3-540-77587-4_118

28. Rajput V, Minkina T, Sushkova S, et al (2020) ZnO and CuO nanoparticles: a threat to soil organisms, plants, and human health. Environ Geochem Health 42:147–158. https://doi.org/10.1007/s10653-019-00317-3
29. Rashid MI, Shahzad T, Shahid M, et al (2017) Zinc oxide nanoparticles affect carbon and nitrogen mineralization of *Phoenix dactylifera* leaf litter in a sandy soil. Journal of hazardous materials 324:298–305
30. Robertson AI, Bunn SE, Boon PI, Walker KF (1999) Sources, sinks and transformations of organic carbon in Australian floodplain rivers. Marine and Freshwater Research 50:813–829
31. Sharma VK (2009) Aggregation and toxicity of titanium dioxide nanoparticles in aquatic environment—A Review. Journal of Environmental Science and Health, Part A 44:1485–1495. https://doi.org/10.1080/10934520903263231
32. Sirelkhatim A, Mahmud S, Seeni A, et al (2015) Review on Zinc Oxide Nanoparticles: Antibacterial Activity and Toxicity Mechanism. Nano-Micro Lett 7:219–242. https://doi.org/10.1007/s40820-015-0040-x
33. Sivakumar P, Lee M, Kim Y-S, Shim MS (2018) Photo-triggered antibacterial and anticancer activities of zinc oxide nanoparticles. J Mater Chem B 6:4852–4871. https://doi.org/10.1039/C8TB00948A
34. Slavin YN, Asnis J, Hńfeli UO, Bach H (2017) Metal nanoparticles: understanding the mechanisms behind antibacterial activity. Journal of nanobiotechnology 15:1–20
35. Sun TY, Bornhöft NA, Hungerbühler K, Nowack B (2016) Dynamic Probabilistic Modeling of Environmental Emissions of Engineered Nanomaterials. Environ Sci Technol 50:4701–4711. https://doi.org/10.1021/acs.est.5b05828
36. Swan CM, Boyero L, Canhoto C (2021) The ecology of plant litter decomposition in stream ecosystems: an overview. Springer.
37. Tank JL, Rosi-Marshall EJ, Griffiths NA, et al (2010) A review of allochthonous organic matter dynamics and metabolism in streams. Journal of the North American Benthological Society 29:118–146
38. Tong T, Fang K, Thomas SA, et al (2014) Chemical interactions between nano-ZnO and nano-TiO2 in a natural aqueous medium. Environmental science & technology 48:7924–7932
39. Venkatasubbu GD, Baskar R, Anusuya T, et al (2016) Toxicity mechanism of titanium dioxide and zinc oxide nanoparticles against food pathogens. Colloids and Surfaces B: Biointerfaces 148:600–606
40. Zhang J, Guo W, Li Q, et al (2018) The effects and the potential mechanism of environmental transformation of metal nanoparticles on their toxicity in organisms. Environ Sci: Nano 5:2482–2499. https://doi.org/10.1039/C8EN00688A
41. Zhang Y, Yin Y, Ma H, et al (2019) Insight into chronic exposure effects of nanosized titanium dioxide on *Typha angustifolia* leaf litter decomposition. Chemosphere 224:680–688. https://doi.org/10.1016/j.chemosphere.2019.02.191

42. Zhao B, Xing P, Wu QL (2017) Microbes participated in macrophyte leaf litters decomposition in freshwater habitat. FEMS Microbiology Ecology 93:. https://doi.org/10.1093/femsec/fix108

Figures

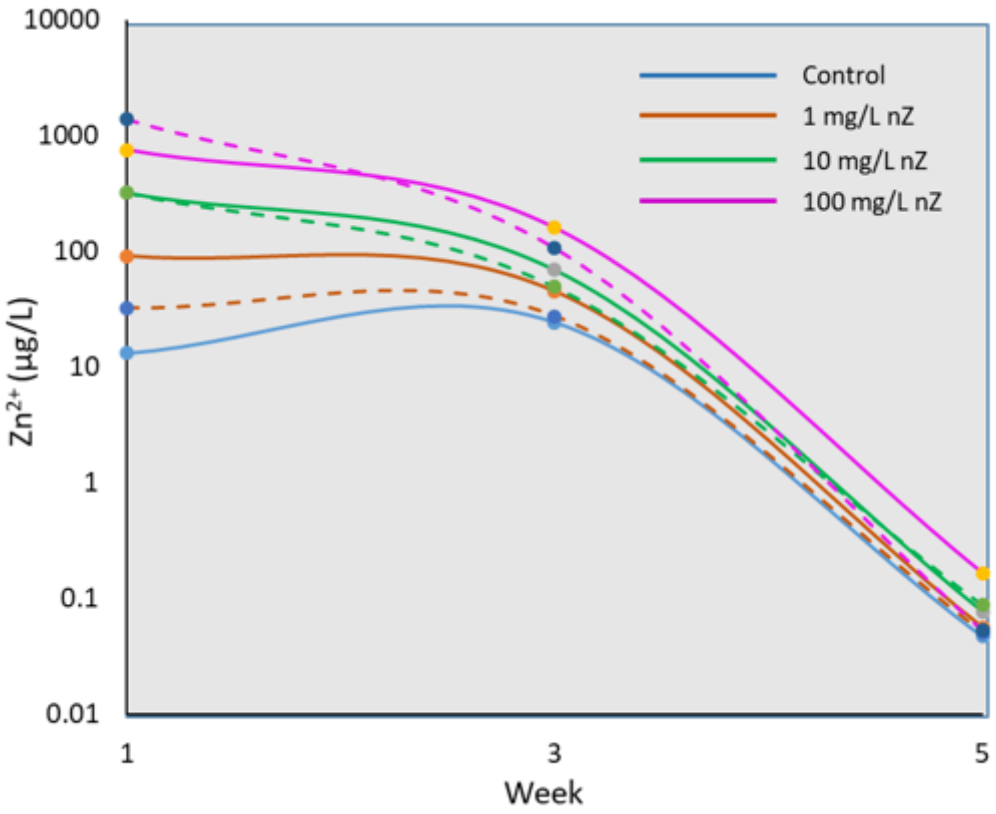

Figure 1

Exp. 1. Change in concentration of Zn^{2+} in different treatments with time. Key: Solid line=nZ without nT. Dashed line= nZ+nT.

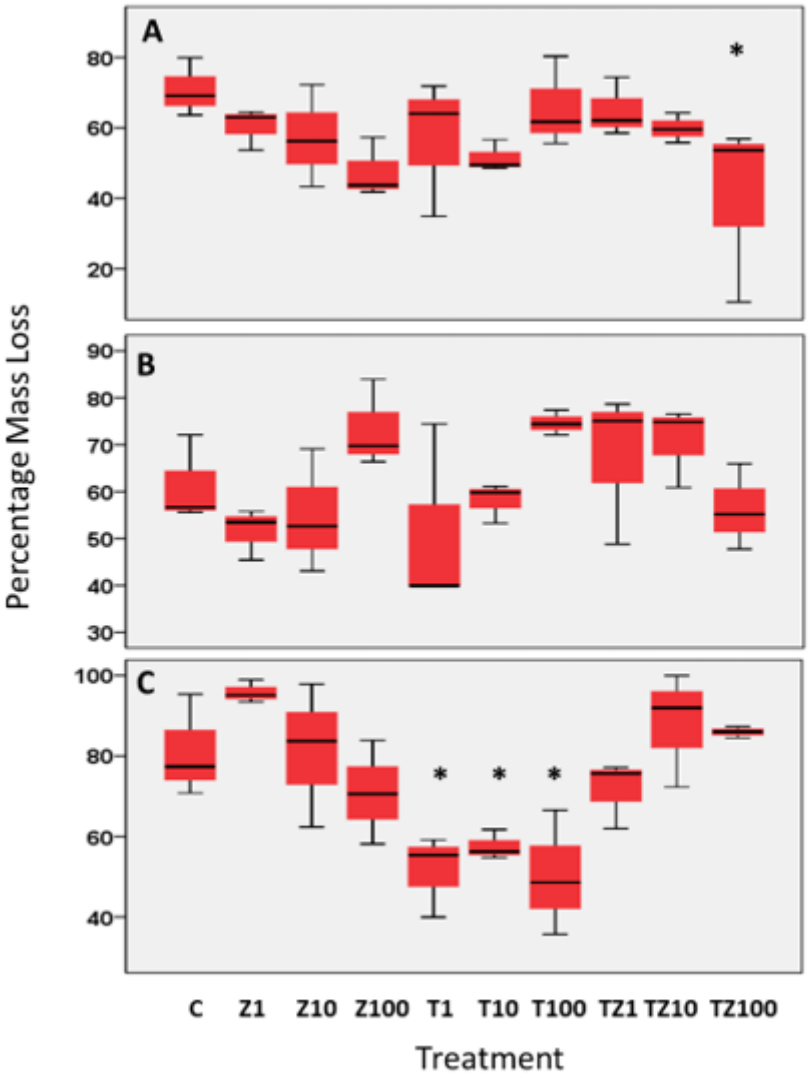

Figure 2

Exp. 1. Effects of nanoparticle treatment of percentage leaf disc mass loss after (A) Two weeks (B) Four weeks (C) Six weeks. (D) Mass loss coefficients. Key: * Significantly different from control (P<0.05).

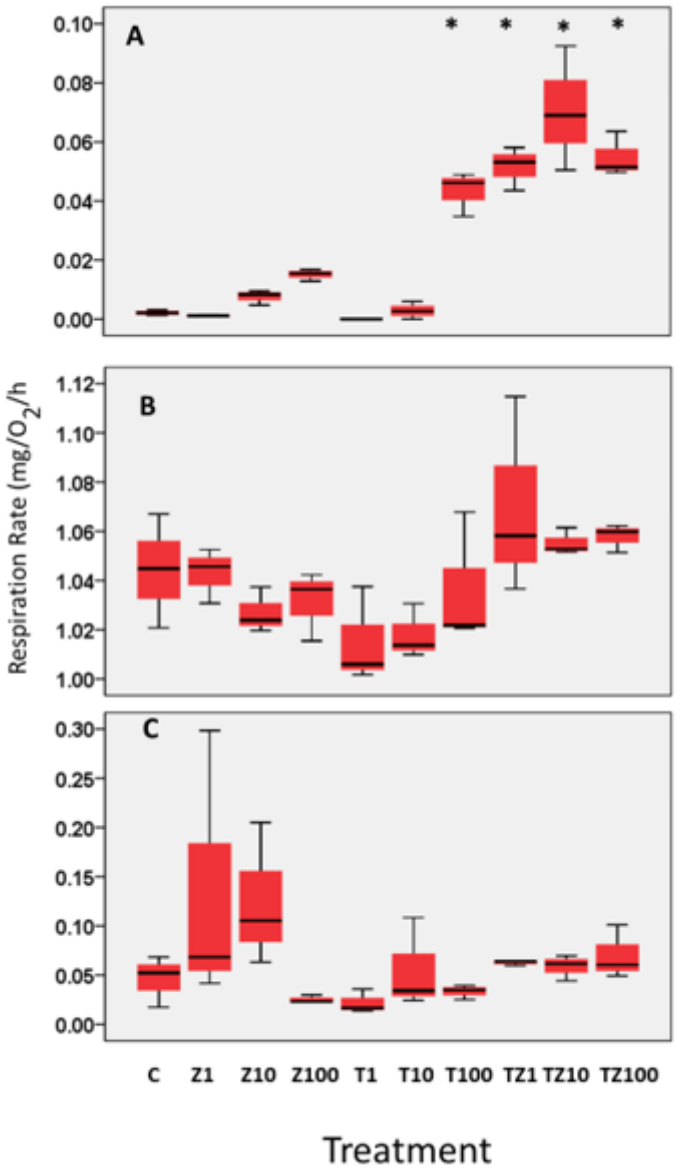

Figure 3

Exp. 1. Effects of nanoparticle treatment on microbial respiration (A) Two weeks (B) Four weeks (C) Six weeks. Key: * Significantly different from control (P<0.05).

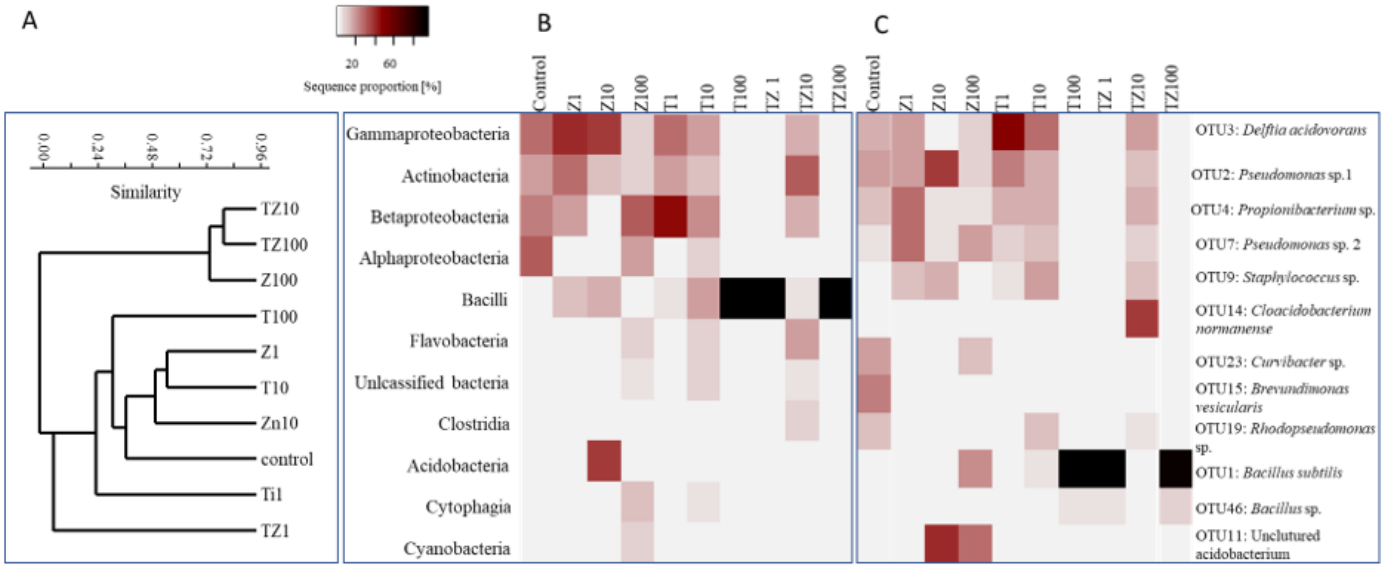

Figure 4

(A) Cluster analysis showing dissimilarity of bacterial communities on leaves based on OTUs. (B) Heat map of relative abundance of dominant phyla (C) Heat map of relative abundance of dominant species.

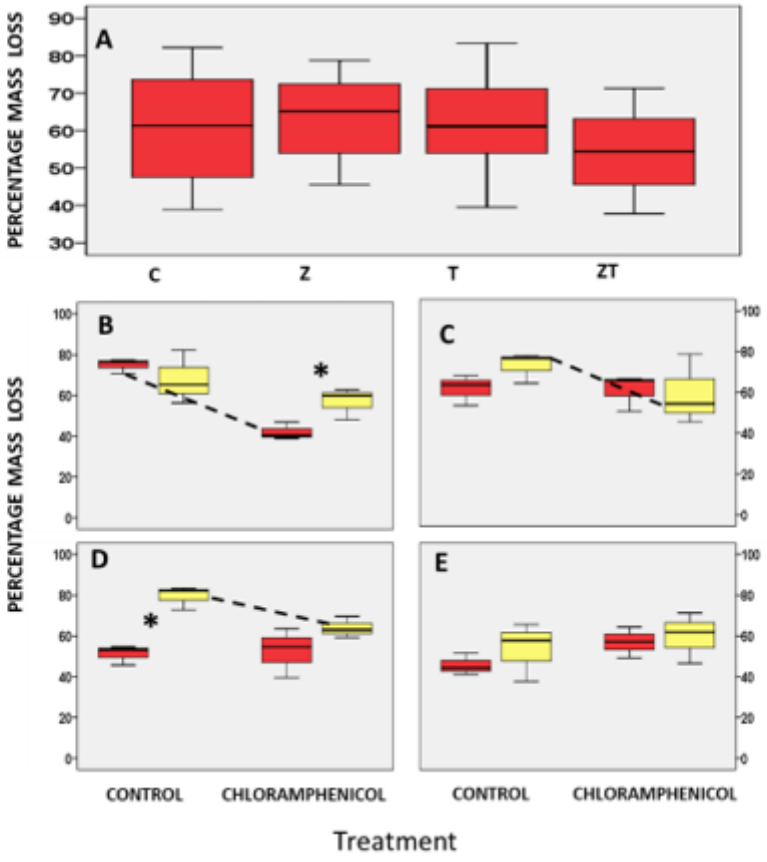

Fig. 5. Exp. 2. (A) Effect of nanoparticle treatment on percentage leaf mass loss averaging over all light/dark and antibiotic treatments. (B-E) Interaction plots of effect of antibiotic and light exposure on leaf mass loss (B) Control (C) nZ 10 mg/L, (D) nT 10 mg/L, (E) nZ+nT 10 mg/L. Key: C=control, Z= nZ 10 mg/L, T=nT 10 mg/L, ZT=nZ+nT 10 mg/L. * P<0.05 between light and dark treatments. -----P<0.05 between +/- chloramphenicol. ■ = Light, ■ =Dark.

Figure 5

See image above for figure legend

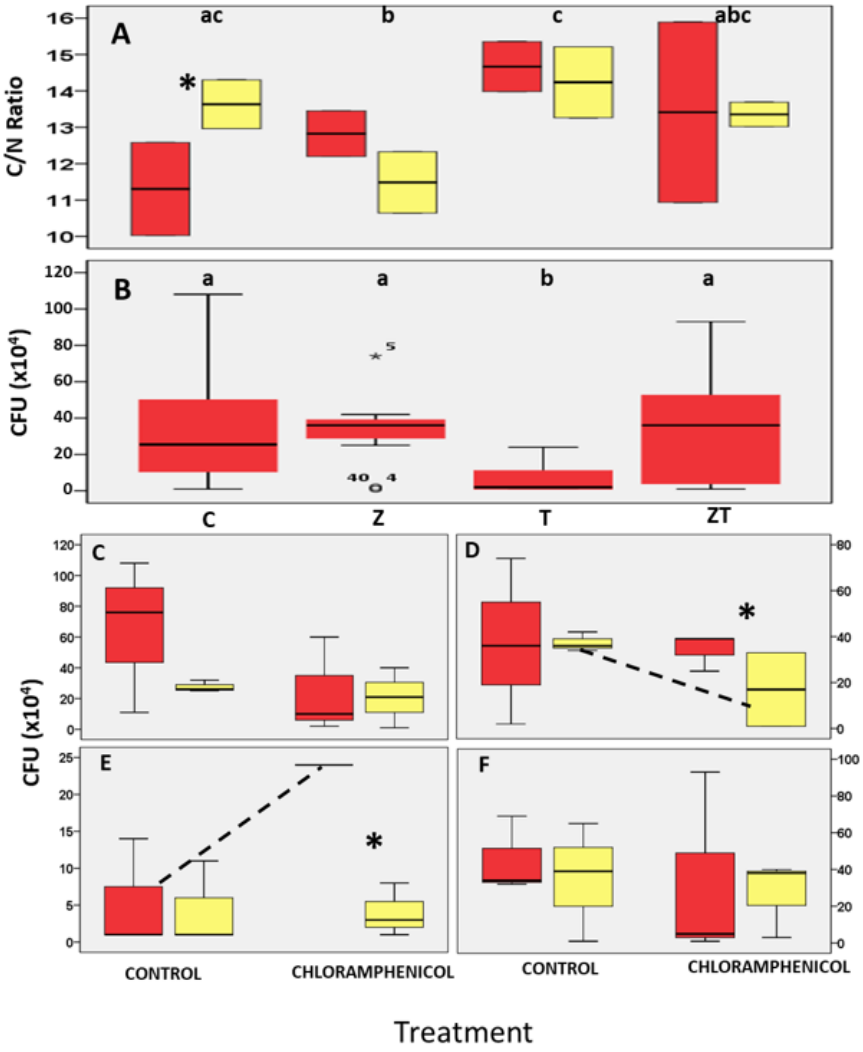

Fig. 6. Exp 2. (A) Effect of nanoparticle treatment and light exposure on leaf mass loss. (B) Effect of nanoparticle treatment on bacterial densities (CFU) averaged over all light/dark and antibiotic treatments. (C-F) Interaction plots of effect of antibiotic and light exposure on leaf mass loss (C) Control (D) nZ 10 mg/L, (E) nT 10 mg/L, (F) nZ+nT 10 mg/L. Key: C=control, Z= nZ 10 mg/L, T=nT 10 mg/L, ZT=nZ+nT 10 mg/L. Common letter above bar indicates no significant difference between treatments ($P>0.05$). * $P<0.05$ between light and dark treatments. -----$P<0.05$ between +/- chloramphenicol. ■ = Light, ■ =Dark.

Figure 6

See image above for figure legend

Supplementary Files

This is a list of supplementary files associated with this preprint. Click to download.

- Appendix1.docx
- Appendix2.docx
- Appendix3Data.xlsx